On the heat flux and entropy produced by thermal fluctuations

Sergio Ciliberto, Alberto Imparato, Antoine Naert, Marius Tanase

On the heat flux and entropy produced by thermal fluctuations

S. Ciliberto[1], A.Imparato[2], A. Naert[1], M. Tanase [1]
1 Laboratoire de Physique,
École Normale Supérieure, C.N.R.S. UMR5672
46 Allée d'Italie, 69364 Lyon, France
and
2 Department of Physics and Astronomy, University of Aarhus
Ny Munkegade, Building 1520, DK–8000 Aarhus C, Denmark

We report an experimental and theoretical analysis of the energy exchanged between two conductors kept at different temperature and coupled by the electric thermal noise. Experimentally we determine, as functions of the temperature difference, the heat flux, the out-of- equilibrium variance and a conservation law for the fluctuating entropy, which we justify theoretically. The system is ruled by the same equations as two Brownian particles kept at different temperatures and coupled by an elastic force. Our results set strong constrains on the energy exchanged between coupled nano-systems held at different temperatures.

The fluctuations of thermodynamics variables play an important role in understanding the out-of-equilibrium dynamics of small systems [1, 2], such as Brownian particles [3–7], molecular motors [8] and other small devices [9]. The statistical properties of work, heat and entropy, have been analyzed, within the context of the fluctuation theorem [10] and stochastic thermodynamics [1, 2], in several experiments on systems in contact with a single heat bath and driven out-of-equilibrium by external forces or fields [3–9]. In contrast, the important case in which the system is driven out-of-equilibrium by a temperature difference and energy exchange is produced only by the thermal noise has been analyzed only theoretically on model systems [11–19] but never in an experiment because of the intrinsic difficulties of dealing with large temperature differences in small systems.

We report here an experimental and theoretical analysis of the statistical properties of the energy exchanged between two conductors kept at different temperature and coupled by the electric thermal noise, as depicted in fig. 1a. This system is inspired by the proof developed by Nyquist [20] in order to give a theoretical explanation of the measurements of Johnson [21] on the thermal noise voltage in conductors. In his proof, assuming thermal equilibrium between the two conductors, he deduces the Nyquist noise spectral density. At that time, well before Fluctuation Dissipation Theorem (FDT), this was the second example, after the Einstein relation for Brownian motion, relating the dissipation of a system to the amplitude of the thermal noise. In this letter we analyze the consequences of removing the Nyquist's equilibrium conditions and we study the statistical properties of the energy exchanged between the two conductors kept at different temperature. This system is probably among the simplest examples where recent ideas of stochastic thermodynamics can be tested but in spite of its simplicity the explanation of the observations is far from trivial. We measure experimentally the heat flowing between the two heath baths, and show that the fluctuating entropy exhibits a conservation law. This system is very general because is ruled by the same equations of two Brownian particles kept at different temperatures and coupled by an elastic force [13, 19]. Thus it gives more insight into the properties of the heat flux produced by mechanical coupling, in the famous Feymann ratchet [22–24] widely studied theoretically [13] but never in an experiment. Therefore our results have implications well beyond the simple system we consider here.

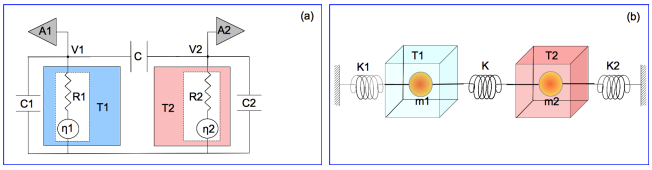

FIG. 1: a) Diagram of the circuit. The resistances R_1 and R_2 are kept at temperature T_1 and $T_2 = 296K$ respectively. They are coupled via the capacitance C. The capacitances C_1 and C_2 schematize the capacitance of the cables and of the amplifier inputs. The voltages V_1 and V_2 are amplified by the two low noise amplifiers A_1 and A_2 [33]. b) The circuit in a) is equivalent to two Brownian particles (m_1 and m_2) moving inside two different heat baths at T_1 and T_2. The two particles are trapped by two elastic potentials of stiffness K_1 and K_2 and coupled by a spring of stiffness K (see text and eqs.3,4) The analogy with the Feymann ratchet can be made by assuming as done in ref.[13] that the particle $m1$ has an asymmetric shape and on average moves faster in one direction than in the other one.

Such a system is sketched in fig.1a). It is constituted by two resistances R_1 and R_2, which are kept at different temperature T_1 and T_2 respectively. These temperatures are controlled by thermal baths and T_2 is kept fixed at

$296K$ whereas T_1 can be set at a value between $296K$ and $88K$ using liquid nitrogen vapor as a circulating coolant. In the figure, the two resistances have been drawn with their associated thermal noise generators η_1 and η_2, whose power spectral densities are given by the Nyquist formula $|\tilde{\eta}_m|^2 = 4k_B R_m T_m$, with $m = 1, 2$ (see eqs.3,4 and ref.[26]). The coupling capacitance C controls the electrical power exchanged between the resistances and as a consequence the energy exchanged between the two baths. No other coupling exists between the two resistances which are inside two separated screened boxes. The quantities C_1 and C_2 are the capacitances of the circuits and the cables. Two extremely low noise amplifiers A_1 and A_2 [33] measure the voltage V_1 and V_2 across the resistances R_1 and R_2 respectively. All the relevant quantities considered in this paper can be derived by the measurements of V_1 and V_2, as discussed below. In the following we will take $C = 100pF, C_1 = 680pF, C_2 = 420pF$ and $R_1 = R_2 = 10M\Omega$, if not differently stated. When $T_1 = T_2$ the system is in equilibrium and exhibits no net energy flux between the two reservoirs. This is indeed the condition imposed by Nyquist to prove his formula, and we use it to check all the values of the circuit parameters. Applying the Fluctuation-Dissipation-Theorem (FDT) to the circuit, one finds the Nyquist's expression for the variance of V_1 and V_2 at equilibrium, which reads $\sigma^2_{m,\mathrm{eq}}(T_m) = k_B T_m (C + C'_m)/X$ with $X = C_2\, C_1 + C\,(C_1 + C_2)$, $m' = 2$ if $m = 1$ and $m' = 1$ if $m = 2$. For example one can check that at $T_1 = T_2 = 296$ K, using the above mentioned values of the capacitances and resistances, the predicted equilibrium standard deviations of V_1 and V_2 are $2.33\mu V$ and $8.16\mu V$ respectively. These are indeed the measured values with an accuracy better than 1%, see ref. [26] for further details on the system calibration.

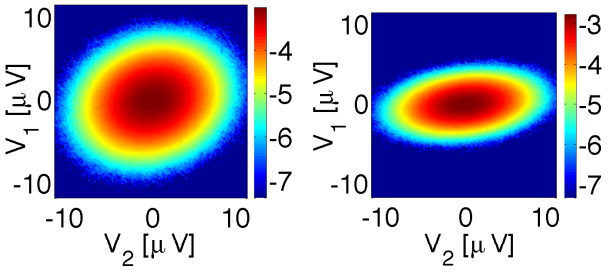

FIG. 2: The joint probability $\log_{10} P(V_1, V_2)$ measured at $T_1 = 296K$ equilibrium (a) and out of equilibrium $T_1 = 88K$(b). The color scale is indicated on the colorbar on the right side.

The important quantity to consider here is the joint probability $P(V_1, V_2)$, which is plotted in fig. 2a) at $T_1 = T_2$ and at fig. 2b) at $T_1 = 88K$. The fact that the axis of the ellipses defining the contours lines of $P(V_1, V_2)$ are inclined with respect to the x and y axis indicates that there is a certain correlation between V_1 and V_2. This correlation, produced by the electric coupling, plays a major role in determining the mean heat flux between the two reservoirs, as we discuss below. The interesting new features occur of course when $T_1 \neq T_2$. The questions that we address for such a system are: What are the heat flux and the entropy production rate ? How the variance of V_1 an V_2 are modified because of the heat flux ? What is the role of correlation between V_1 and V_2? We will see that these questions are quite relevant and have no obvious answers because of the statistical nature of the energy transfer.

We consider the electric power dissipated in the resistance R_m with $m = 1, 2$ which reads $\dot{Q}_m = V_m\, i_m$ where i_m is the current flowing in the resistance m. The integral of the power over a time τ is the total energy Q_m, dissipated by the resistance in this time interval, i.e. $Q_{m,\tau} = \int_t^{t+\tau} i_m\, V_m\, dt$. All the voltages V_m and currents i_m can be measured: indeed we have $i_m = i_C - i_{C_m}$ where $i_C = C\frac{d(V_2 - V_1)}{dt}$ is the current flowing in the capacitance C, and $i_{C_m} = C_m \frac{dV_m}{dt}$ is the current flowing in C_m. Thus rearranging the terms one finds that $Q_{m,\tau} = W_{m,\tau} - \Delta U_{m,\tau}$ where $W_{1,\tau} = \int_t^{t+\tau} C\, V_1 \frac{dV_2}{dt} dt$, $W_{2,\tau} = \int_t^{t+\tau} C V_2 \frac{dV_1}{dt} dt$ and $\Delta U_{m,\tau} = \frac{(C_m + C)}{2}(V_m(t+\tau)^2 - V_m(t)^2)$ is the potential energy change of the circuit m in the time τ. Notice that W_m are the terms responsible for the energy exchange since they couple the fluctuations of the two circuits. The quantities $W_{1,\tau}$ and $W_{2,\tau}$ can be identified as the work performed by the circuit 2 on 1 and vice-versa [25, 27, 30], respectively. Thus, the quantity $Q_{1,\tau}$ ($Q_{2,\tau}$) can be interpreted as the heat flowing from the reservoir 2 to the reservoir 1 (from 1 to 2), in the time interval τ, as an effect of the temperature difference. As the two variables V_m are fluctuating voltages all the other quantities also fluctuate. In fig. 3a) we show the probability density function $P(Q_{1,\tau})$, at various temperatures: we see that $Q_{1,\tau}$ is a strongly fluctuating quantity, whose $P(Q_{1,\tau})$ has long exponential tails.

Notice that although for $T_1 < T_2$ the mean value of $Q_{1,\tau}$ is positive, instantaneous negative fluctuations can occur, i.e., sometimes the heat flux is reversed. The mean values of the dissipated heats are expected to be linear functions of the temperature difference $\Delta T = T_2 - T_1$, i.e. $\langle Q_{1,\tau} \rangle = A\, \tau\, \Delta T$, where A is a parameter dependent quantity, that can be obtained explicitly from eqs. 3 and 4 below. This relation is confirmed by our experimental

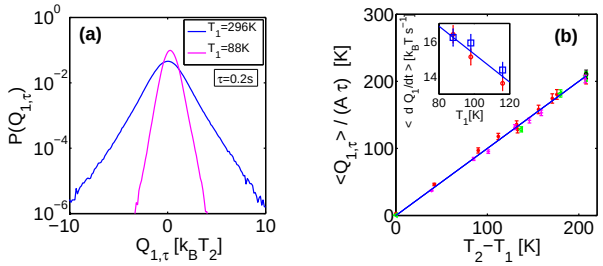

FIG. 3: a) The probability $P(Q_{1,\tau})$ measured at $T_1 = 296K$ (blue line) equilibrium and $T_1 = 88K$ (magenta line) out of equilibrium. Notice that the peak of the $P(Q_{1,\tau})$ is centered at zero at equilibrium and shifted towards a positive value out of equilibrium. The amount of the shift is very small and is $\sim k_B(T_2 - T_1)$. b) The measured mean value of $\langle Q_{1,\tau}\rangle$ is a linear function of $(T_2 - T_1)$. The red points correspond to measurements performed with the values of the capacitance C_1, C_2, C given in the text and $\tau = 0.2s$. The other symbols and colors pertain to different values of these capacitance and other τ: (black $\circ$) $\tau = 0.4s, C = 1000pF$, (green $\triangleleft$) $\tau = 0.1s, C = 100pF$, (magenta $+$) $\tau = 0.5s, C = 100pF$. The values of $\langle Q_{1,\tau}\rangle$ have been rescaled by the parameter dependent theoretical prefactor A, which allows the comparison of different experimental configurations. The continuous blue line with slope 1 is the theoretical prediction of eq. 7. In the inset the values of $< \dot{Q}_1 >$ (at $C = 1000pF$) directly measured using $P(Q_1)$ (blue square) are compared with those (red circles) obtained from the equality $< \dot{Q}_1 >= (\sigma_1^2 - \sigma_{1,\mathrm{eq}}^2)/R_1$, as discussed in the text.

results, as shown in fig. 3b. Furthermore, the mean values of the dissipated heat satisfy the equality $\langle Q_2\rangle = -\langle Q_1\rangle$, corresponding to an energy conservation principle: the power extracted from the bath 2 is dissipated into the bath 1 because of the electric coupling. This mean flow produces a change of the variances $\sigma_m^2(T_m)$ of V_m with respect to the equilibrium value $\sigma_{m,\mathrm{eq}}^2(T_m)$, that is the equilibrium value measured when the two baths are at the same temperature T_m. Specifically we find $\sigma_m^2(T_m) = \sigma_{m,\mathrm{eq}}^2(T_m) + < \dot{Q}_m > R_m$ which is an extension to two temperatures of the Harada-Sasa relation [34] (see also ref.[26] for a theoretical proof of this experimental result). This result is shown in the inset of fig. 3b) where the values of $\left\langle \dot{Q}_m \right\rangle$ directly estimated from the experimental data (using the steady state $P(Q_m)$) are compared with those obtained from the difference of the variances of V_1 measured in equilibrium and out-of-equilibrium. The values are comparable within error bars and show that the out-of-equilibrium variances are modified only by the heat flux. It is now important to analyze the entropy produced by the total system, circuit

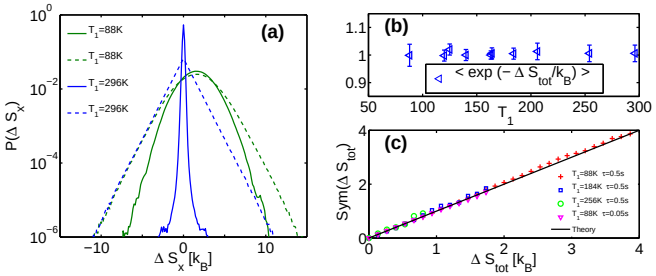

FIG. 4: a) The probability $P(\Delta S_r)$ (dashed lines) and $P(\Delta S_{tot})$ (continuous lines) measured at $T_1 = 296K$ (blue line) which corresponds to equilibrium and $T_1 = 88K$ (green lines) out of equilibrium. Notice that both distributions are centered at zero at equilibrium and shifted towards positive value in the out-of-equilibrium. b) $\langle \exp(-\Delta S_{tot})\rangle$ as a function of T_1 at two different $\tau = 0.5s$ and $\tau = 0.1s$. c) Symmetry function $\mathrm{Sym}(\Delta \mathrm{S_{tot}}) = \log[\mathrm{P}(\Delta \mathrm{S_{tot}})/\mathrm{P}(-\Delta \mathrm{S_{tot}})]$ as a function of ΔS_{tot}. The black straight line of slope 1 corresponds to the theoretical prediction.

plus heat reservoirs. We consider first the entropy $\Delta S_{r,\tau}$ due to the heat exchanged with the reservoirs, which reads $\Delta S_{r,\tau} = Q_{1,\tau}/T_1 + Q_{2,\tau}/T_2$. This entropy is a fluctuating quantity as both Q_1 and Q_2 fluctuate, and its average in a time τ is $\langle \Delta S_{r,\tau}\rangle = \langle Q_{r,\tau}\rangle (1/T_1 - 1/T_2) = A\tau(T_2 - T_1)^2/(T_2\, T_1)$. However the reservoir entropy $\Delta S_{r,\tau}$ is not the only component of the total entropy production: one has to take into account the entropy variation of the system, due to its dynamical evolution. Indeed, the state variables V_m also fluctuate as an effect of the thermal noise, and thus, if one measures their values at regular time interval, one obtains a "trajectory" in the phase space $(V_1(t), V_2(t))$. Thus, following Seifert [28], who developed this concept for a single heat bath, one can introduce a trajectory entropy for the evolving system $S_s(t) = -k_B \log P(V_1(t), V_2(t))$, which extends to non-equilibrium systems the standard Gibbs entropy concept. Therefore, when evaluating the total entropy production, one has to take into

account the contribution over the time interval τ of

$$\Delta S_{s,\tau} = -k_B \log\left[\frac{P(V_1(t+\tau), V_2(t+\tau))}{P(V_1(t), V_2(t))}\right]. \quad (1)$$

It is worth noting that the system we consider is in a non-equilibrium steady state, with a constant external driving ΔT. Therefore the probability distribution $P(V_1, V_2)$ (as shown in fig. 2b)) does not depend explicitly on the time, and $\Delta S_{s,\tau}$ is non vanishing whenever the final point of the trajectory is different from the initial one: $(V_1(t+\tau), V_2(t+\tau)) \neq (V_1(t), V_2(t))$. Thus the total entropy change reads $\Delta S_{tot,\tau} = \Delta S_{r,\tau} + \Delta S_{s,\tau}$, where we omit the explicit dependence on t, as the system is in a steady-state as discussed above. This entropy has several interesting features. The first one is that $\langle \Delta S_{s,\tau} \rangle = 0$, and as a consequence $\langle \Delta S_{tot} \rangle = \langle \Delta S_r \rangle$ which grows with increasing ΔT. The second and most interesting result is that independently of ΔT and of τ, the following equality always holds:

$$\langle \exp(-\Delta S_{tot}/k_B) \rangle = 1, \quad (2)$$

for which we find both experimental evidence, as discussed in the following, and provide a theoretical proof in ref. [26]. Equation (2) represents an extension to two temperature sources of the result obtained for a system in a single heat bath driven out-of-equilibrium by a time dependent mechanical force [6, 28] and our results provide the first experimental verification of the expression in a system driven by a temperature difference. Eq. (2) implies that $\langle \Delta S_{tot} \rangle \geq 0$, as prescribed by the second law. From symmetry considerations, it follows immediately that, at equilibrium ($T_1 = T_2$), the probability distribution of ΔS_{tot} is symmetric: $P_{eq}(\Delta S_{tot}) = P_{eq}(-\Delta S_{tot})$. Thus Eq. (2) implies that the probability density function of ΔS_{tot} is a Dirac δ function when $T_1 = T_2$, i.e. the quantity ΔS_{tot} is rigorously zero in equilibrium, both in average and fluctuations, and so its mean value and variance provide a measure of the entropy production. The measured probabilities $P(\Delta S_r)$ and $P(\Delta S_{tot})$ are shown in fig. 4a). We see that $P(\Delta S_r)$ and $P(\Delta S_{tot})$ are quite different and that the latter is close to a Gaussian and reduces to a Dirac δ function in equilibrium, i.e. $T_1 = T_2 = 296K$ (notice that, in fig.4a, the small broadening of the equilibrium $P(\Delta S_{tot})$ is just due to unavoidable experimental noise and discretization of the experimental probability density functions). The experimental measurements satisfy eq. (2) as it is shown in fig. 4b). It is worth to note that eq. (2) implies that $P(\Delta S_{tot})$ should satisfy a fluctuation theorem of the form $\log[P(\Delta S_{tot})/P(-\Delta S_{tot})] = \Delta S_{tot}/k_B, \ \forall \tau, \Delta T$, as discussed extensively in reference [1, 29]. We clearly see in fig.4c) that this relation holds for different values of the temperature gradient. Thus this experiment clearly establishes a relationship between the mean and the variance of the entropy production rate in a system driven out-of-equilibrium by the temperature difference between two thermal baths coupled by electrical noise. Because of the formal analogy with Brownian motion the results also apply to mechanical coupling as discussed in the following.

We will now give a theoretical interpretation of the experimental observations. This will allow us to show the analogy of our system with two interacting Brownian particles coupled to two different temperatures, see fig. 1-b). Let q_m ($m = 1, 2$) be the charges that have flowed through the resistances R_m, so the instantaneous current flowing through them is $i_m = \dot{q}_m$. A circuit analysis shows that the equations for the charges are:

$$R_1 \dot{q}_1 = -q_1 \frac{C_2}{X} + (q_2 - q_1)\frac{C}{X} + \eta_1 \quad (3)$$

$$R_2 \dot{q}_2 = -q_2 \frac{C_1}{X} + (q_1 - q_2)\frac{C}{X} + \eta_2 \quad (4)$$

where η_m is the usual white noise: $\langle \eta_i(t)\eta_j(t') \rangle = 2\delta_{ij} k_B T_i R_j \delta(t - t')$. The relationships between the measured voltages and the charges are:

$$q_1 = (V_1 - V_2)\, C + V_1\, C_1 \quad (5)$$

$$q_2 = (V_1 - V_2)\, C - V_2\, C_2 \quad (6)$$

Eqs. 3 and 4 are the same of those for the two coupled Brownian particles sketched in fig.1b) by considering q_m the displacement of the particle m, i_m its velocity, $K_m = 1/C_m$ the stiffness of the spring m, $K = 1/C$ the coupling spring and R_m the viscosity. With this analogy we see that our definition of the heat flow Q_m corresponds exactly to the work performed by the viscous forces and by the bath on the particle m, and it is consistent with the stochastic thermodynamics definition [1, 25, 30–32]. Thus our theoretical analysis and the experimental results apply to both interacting mechanical and electrical systems coupled to baths at different temperatures. Starting from eqs. (3)-(4), we can prove (see ref. [26]) that eq.2 is an exact result and that the average dissipated heat rate is

$$\left\langle \dot{Q}_1 \right\rangle = A\,(T_2 - T_1) = \frac{C^2 \Delta T}{XY}, \quad (7)$$

with $Y = [(C_1 + C)R_1 + (C_2 + C)R_2]$ and $A = C^2/(X\,Y)$ is the parameter used to rescale the data in fig. 3b).

To conclude we have studied experimentally the statistical properties of the energy exchanged between two heat baths at different temperature which are coupled by electric thermal noise. We have measured the heat flux, the entropy production rate and we have shown the existence of a conservation law for entropy which imposes the existence of a fluctuation theorem which is not asymptotic in time. Our results, which are theoretically proved, are very general since the electric system considered here is ruled by the same equations as for two Brownian particles, held at different temperatures and mechanically coupled. Therefore these results set precise constraints on the energy exchanged between coupled nano and micro-systems held at different temperatures. We finally mention that for the quantity W_i an asymptotic fluctuation theorem can be proved both experimentally and theoretically, and this will be the subject of a paper in preparation.

[1] U. Seifert *Rep. Progr. Phys.* **75**, 126001, (2012).
[2] Sekimoto, K. *Stochastic Energetics.* (Springer, 2010).
[3] Blickle V., Speck T., Helden L., Seifert U., and Bechinger C. *Phys. Rev. Lett.* **96**, 070603 (2006).
[4] Jop, P., Petrosyan A. and Ciliberto S. *EPL* **81**, 50005 (2008).
[5] Gomez-Solano, J. R., Petrosyan, A., Ciliberto, S. Chetrite, R. and Gawedzki K. *Phys. Rev. Lett* 103, 040601 (2009).
[6] G. M. Wang, E. M. Sevick, E. Mittag, D. J. Searles, and D. J. Evans, *Phys. Rev. Lett.*, **89**: 050601 (2002).
[7] J. Mehl, B. Lander, C. Bechinger, B. Blicke and U. Seifert, Phys. Rev. Lett. **108**, 220601 (2012).
[8] K. Hayashi, H. Ueno, R. Iino, H. Noji, Phys. Rev. Lett. 104, 218103 (2010)
[9] S Ciliberto, S Joubaud and A Petrosyan J. Stat. Mech., P12003 (2010).
[10] D. J. Evans *et al.*, Phys. Rev. Lett. **71**, 2401 (1993); G. Gallavotti, E. G. D. Cohen, J. Stat. Phys. **80**, 931 (1995).
[11] T. Bodinau, B. Deridda, Phy.Rev. Lett 92, 180601 (2004).
[12] C. Jarzynski and D. K. Wójcik Phys. Rev. Lett. 92, 230602 (2004).
[13] C. Van den Broeck, R. Kawai and P. Meurs, Phys. Rev. Lett 93, 090601 (2004).
[14] P Visco, J. Stat. Mech., page P06006, (2006).
[15] K. Saito and A. Dhar Phys. Rev. Lett. 99, 180601 (2007).
[16] D. Andrieux, P. Gaspard, T. Monnai, S. Tasaki, New J. Phys. 11, 043014 (2009).
[17] Evans D. , Searles D. J. Williams S. R., J. Chem. Phys. 132, 024501 2010.
[18] M. Campisi, P. Talkner, P. Hanggi, Rev. Mod. Phys. 83, 771 (2011)
[19] A. Crisanti, A. Puglisi, and D. Villamaina, Phys. Rev. E 85, 061127 (2012)
[20] H. Nyquist, Phys. Rev. 32, 110 (1928)
[21] J. Johnson, Phys. Rev. 32, 97 (1928)
[22] R. P. Feynman, R. B. Leighton, and M. Sands, The Feynman Lectures on Physics I (Addison-Wesley, Reading, MA, 1963), Chap. 46.
[23] M. v. Smoluchowski, Phys. Z. 13, 1069 (1912).
[24] D. Abbott, B. R. Davis, and J. M. R. Parrondo, AIP Conf. Proc. 511, 213 (2000).
[25] Sekimoto K, Prog. Theor. Phys. Suppl. 130, 17, (1998)
[26] Supplementary Material.
[27] N. Garnier, S. Ciliberto, Phys. Rev. E, 71, 060101(R) (2005)
[28] U. Seifert, *Phys. Rev. Lett.*, **95**: 040602 (2005).
[29] M. Esposito, C. Van den Broeck, *Phys. Rev. Lett.*, **104**, 090601 (2010).
[30] R. van Zon, S. Ciliberto, E. G. D. Cohen,*Phys. Rev. Lett.* **92**: 130601 (2004).
[31] A. Imparato, L. Peliti, G. Pesce, G. Rusciano, A. Sasso, *Phys. Rev. E*, **76**: 050101R (2007).
[32] H. C. Fogedby, A. Imparato, *J. Stat. Mech.* P04005 (2012).
[33] G. Cannatá, G. Scandurra, C. Ciofin,Rev. Scie. Instrum. 80,114702 (2009).
[34] Harada T. Sasa S.-I.,Phys. Rev. Lett.,95,130602(2005).

On the heat flux and entropy produced by thermal fluctuations: Supplementary information

S. Ciliberto[1], A.Imparato[2], A. Naert[1], M. Tanase [1]
1 Laboratoire de Physique,
École Normale Supérieure, C.N.R.S. UMR5672
46 Allée d'Italie, 69364 Lyon, France
and
2 Department of Physics and Astronomy, University of Aarhus
Ny Munkegade, Building 1520, DK–8000 Aarhus C, Denmark

I. EXPERIMENTAL DETAILS

A. Experimental set up

The electric systems and amplifiers are inside a Faraday cage and mounted on a floating optical table to reduce mechanical and acoustical noise. The resistance R_1, which is cooled by liquid Nitrogen vapors, changes of less than 0.1% in the whole temperature range. Its temperature is measured by a PT1000 which is inside the same shield of R_1. The signal V_1 and V_2 are amplified by two custom designed JFET amplifiers [1] with an input current of $1pA$ and a noise of $0.7nV\sqrt{Hz}$ at frequencies larger than $1Hz$ and increases at $8nV\sqrt{Hz}$ at $0.1Hz$. The resistances $R1$ and $R2$ have been used as input resistances of the amplifiers. The two signals V_1 and V_2 are amplified 10^4 times and the amplifier outputs are filtered (at $4KHz$ to avoid aliasing) and acquired at $8KHz$ by 24 bits-ADC. We used different sets of C_1, C_2 and C. The values of $C1$ and $C2$ are essentially set by the input capacitance of the amplifiers and by the cable length $680pF < C1 < 780pF$ and $400pF < C_2 < 500pF$. Instead C has been changed from $100pF$ to $1000pF$. The system has always been calibrated in equilibrium at $T_1 = T_2 = 296K$ using the FDT and estimating the spectrum using the values of the capacitances, see next sections.

B. Noise spectrum of the amplifiers

The noise spectrum of the amplifiers A_1 and A_2 (Fig.1 of the main text), measured with a short circuit at the inputs, is plotted in fig.S.1a) and compared with the spectrum Sp_1 of V_1 at $T_1 = 88K$. We see that the useful signal is several order of magnitude larger than the amplifiers noise.

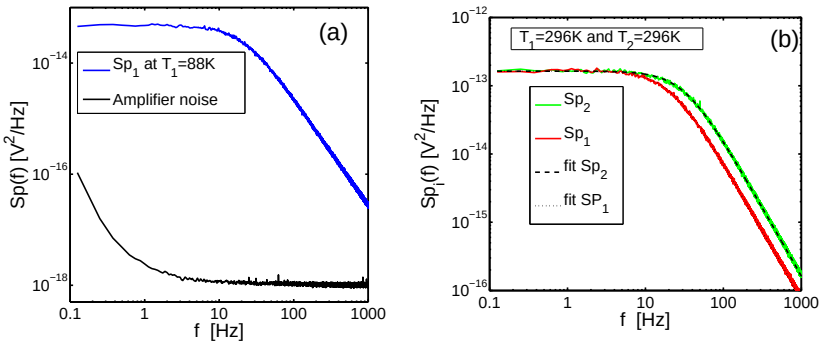

FIG. S.1: a) The power spectra Sp_1 of V_1 measured at $T_1 = 88K$ (blue line) ($C = 100pF, C_1 = 680pF, C_2 = 430pF$) is compared to the spectrum of the amplifier noise. b) The equilibrium spectra Sp_1(red line) and Sp_2 (green line) measured at $T_1 = T_2 = 296K$ are compared with prediction of eqs.S.1 and S.2 in order to check the values of the capacitances (C_1, C_2).

C. Check of the calibration

The equilibrium spectra of V_1 and V_2 at $T_1 = T_2$ used for calibration of the capacitances are:

$$S_1(\omega) = \frac{4k_B T_1\, R_1[1+\omega^2(C^2R_1R_2+R_2^2(C_2+C)^2)]}{(1-\omega^2\, X\, R_1R_2)^2+\omega^2 Y^2} \tag{S.1}$$

$$S_2(\omega) = \frac{4k_B T_2\, R_2[1+\omega^2(C^2R_1R_2+R_1^2(C_1+C)^2)]}{(1-\omega^2\, X\, R_1R_2)^2+\omega^2 Y^2} \tag{S.2}$$

where $Y = [(C_1+C)R_1+(C_2+C)R_2]$ and $X = C_2\, C_1 + C\,(C_1\, + C_2)$. This spectra can be easily obtained by applying FDT to the circuit of fig.1 in the main text.

The two computed spectra are compared to the measured ones in fig. S.1a). This comparison allows us to check the values of the capacitances C_1 and C_2 which depend on the cable length. We see that the agreement between the prediction and the measured power spectra is excellent and the global error on calibration is of the order of 1%. This corresponds exactly to the case discussed by Nyquist in which the two resistances at the same temperature are exchanging energy via an electric circuit (C in our case).

D. The power spectra of V_1 and V_2 out-of-equilibrium

When $T_1 \neq T_2$ the power spectra of V_1 and V_2 are:

$$S_1(\omega) = \frac{4k_B T_1\, R_1[1+\omega^2(C^2R_1R_2+R_2^2(C_2+C)^2)]}{(1-\omega^2\, X\, R_1R_2)^2+\omega^2 Y^2} + \frac{4k_B(T_2-T_1)\,\omega^2\, C^2R_1^2R_2}{(1-\omega^2\, X\, R_1R_2)^2+\omega^2 Y^2} \tag{S.3}$$

$$S_2(\omega) = \frac{4k_B T_2\, R_2[1+\omega^2(C^2R_1R_2+R_1^2(C_1+C)^2)]}{(1-\omega^2\, X\, R_1R_2)^2+\omega^2 Y^2} + \frac{4k_B(T_1-T_2)\,\omega^2\, C^2R_2^2R_1}{(1-\omega^2\, X\, R_1R_2)^2+\omega^2 Y^2} \tag{S.4}$$

These equations have been obtained by Fourier transforming eqs. S.7,S.8, solving for $\tilde{V}_1(\omega)$ and $\tilde{V}_2(\omega)$ and computing the modula. The integral of eqs. S.3 and S.4 gives the variances eq. S.24 directly computed from the distributions.

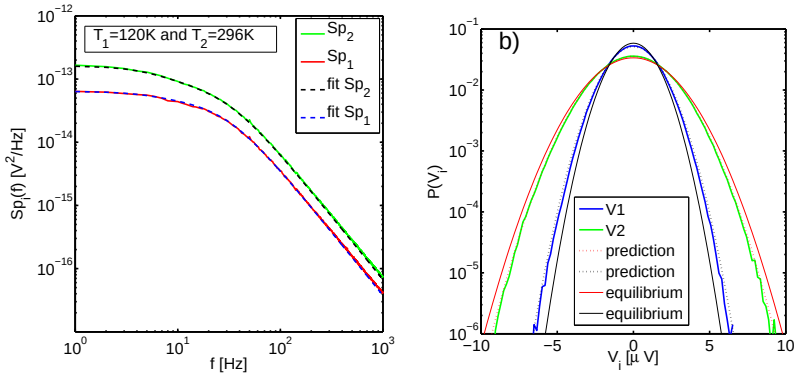

FIG. S.2: a) The power spectra Sp_1 of V_1 and Sp_2 of V_2 measured at $T_1 = 120K$ and $T_2 = 296K$ ($C = 100pF, C_1 = 680pF, C_2 = 430pF$) are compared with the prediction of eq.S.3 and S.4 (dashed lines) b) The corresponding Probability Density Function $P(V_1)$ of V_1 (green line) and $P(V_2)$ of V_2 (blue line) measured at $T_1 = 120K$ and $T_2 = 296K$. Dotted lines are the out-of-equilibrium PDF, whose variance is estimated from the measure of the heat flux (see fig.3 in the main text) and eq.S.24 in the following section. The continuous red line is the equilibrium $P(V_2)$ at $T_1 = 296K$ and the black continuous line corresponds to the equilibrium $P(V_1)$ at $T_2 = 120K$.

E. Measure of the equilibrium variance of V_1 as a function of T_1

This measure is necessary to estimate $< Q_1 >$ starting from the measurement of the variances as explained in fig.4 of the main text. We first measure $\sigma^2_{m,\mathrm{eq}}(T1)$ at $T_1 = T_2 = 296K$. Indeed in equilibrium the variance must be proportional to

$T_1 = T_2$, i.e. $\sigma^2_{m,\mathrm{eq}}(T_1) = \alpha_m T_1$, and from the equilibrium measurements at $T_1 = T_2$ one gets the proportionality constant $\alpha_m = \sigma^2_{m,\mathrm{eq}}(T_1)/T_1$. Thus when $T_1 < T_2$ one can estimate the values of the equilibrium variances $\sigma^2_{m,\mathrm{eq}}(T1) = \alpha_m\, T_1$. As explained in the main text $< \dot{Q}_1 >= (\sigma_1^2(T1) - \sigma^2_{m,\mathrm{eq}}(T1))/R_1$. In fig. S.2b) we compare the measured PDF of V_1 and V_2 with the equilibrium and the out-of-equilibrium distributions as computed by using the theoretical predictions eq.S.24 for the variance.

II. DYNAMICAL EQUATIONS FOR V_m AND Q_m.

We want to describe, with a set of coupled Langevin equations, the dynamical evolution of both the electric and thermodynamic variables for the circuit in fig. 1 of the main text. For this purpose we write the Langevin equations governing the dynamical evolutions for the voltages across the circuit:

$$(C_1 + C)\dot{V}_1 = C\dot{V}_2 + \frac{1}{R_1}(\eta_1 - V_1) \tag{S.5}$$

$$(C_2 + C)\dot{V}_2 = C\dot{V}_1 + \frac{1}{R_2}(\eta_2 - V_2) \tag{S.6}$$

where we have substituted eqs. (5)-(6) into eqs. (3)-(4) in the main text. We rearrange these equations in a standard form, and obtain

$$\dot{V}_1 = f_1(V_1, V_2) + \sigma_{11}\eta_1 + \sigma_{12}\eta_2 = f_1(V_1, V_2) + \xi_1 \tag{S.7}$$

$$\dot{V}_2 = f_2(V_1, V_2) + \sigma_{21}\eta_1 + \sigma_{22}\eta_2 = f_2(V_1, V_2) + \xi_2 \tag{S.8}$$

where the "forces" acting on the circuits read

$$f_1(V_1, V_2) = \alpha_1 V_1 + \alpha_2 V_2 = -\frac{C_2 R_2 V_1 + C(R_2 V_1 + R_1 V_2)}{[C_2 C + C_1(C_2 + C)]R_1 R_2}, \tag{S.9}$$

$$f_2(V_1, V_2) = \gamma_1 V_1 + \gamma_2 V_2 = -\frac{C_1 R_1 V_2 + C(R_2 V_1 + R_1 V_2)}{[C_2 C + C_1(C_2 + C)]R_1 R_2}, \tag{S.10}$$

the coefficients σ_{ij} read

$$\begin{aligned} \sigma_{11} &= \frac{C_2 + C}{XR1} \\ R_2\sigma_{12} &= R_1\sigma_{21} = \frac{C}{X} \\ \sigma_{22} &= \frac{C_1 + C}{XR_2}, \end{aligned}$$

and the noises ξ_i introduced in eqs. (S.7)-(S.8) are now correlated $\langle \xi_i \xi'_j \rangle = 2\theta_{ij}\delta(t - t')$, where

$$\theta_{11} = \frac{T_1(C_2 + C)^2}{R_1(C_2 C + C_1(C_2 + C))^2} + \frac{T_2 C^2}{R_2(C_2 C + C_1(C_2 + C))^2}, \tag{S.11}$$

$$\theta_{12} = \frac{T_1(C(C_2 + C))}{R_1(C_2 C + C_1(C_2 + C))^2} + \frac{T_2(C(C_1 + C))}{R_2(C_2 C + C_1(C_2 + C))^2}, \tag{S.12}$$

$$\theta_{22} = \frac{T_1 C^2}{R_1(C_2 C + C_1(C_2 + C))^2} + \frac{T_2(C_1 + C)^2}{R_2(C_2 C + C_1(C_2 + C))^2}, \tag{S.13}$$

and $\theta_{12} = \theta_{21}$. We now notice that the rate of the dissipated heat in circuit m reads

$$\dot{Q}_m = V_m i_m = \frac{V_m}{R_m}(V_m - \eta_m) = V_m\left[(C_m + C)\dot{V}_m - C\dot{V}_{m'}\right], \tag{S.14}$$

where $m' = 2$ if $m = 1$, and $m' = 1$ if $m = 2$. The rightmost equality in eq. (S.14) follows immediately from eqs. (S.5)-(S.6). So one has a formalism where both the voltages and the dissipated heats are described as stochastic processes, driven by the thermal noises η_m.

III. PROBABILITY DISTRIBUTION FUNCTION FOR THE VOLTAGES

We now study the joint probability distribution function (PDF) $P(V_1, V_2, t)$, that the system at time t has a voltage drop V_1 across the resistor R_1 and a voltage drop V_2 across the resistor R_2. As the time evolution of V_1 and V_2 is described by the Langevin equations (S.7)-(S.8), it can be proved that the time evolution of $P(V_1, V_2, t)$ is governed by the Fokker-Planck equation [2]

$$\begin{aligned}\partial_t P(V_1, V_2, Q_1, t) = L_0 P(V_1, V_2, t) \;=\; & -\frac{\partial}{\partial V_1}\left(f_1 P\right) - \frac{\partial}{\partial V_2}\left(f_2 P\right) + \theta_{11}\frac{\partial^2}{\partial V_1^2}P + \theta_{22}\frac{\partial^2}{\partial V_2^2}P \\ & + 2\theta_{12}\frac{\partial^2}{\partial V_1 \partial V_2}P \end{aligned} \tag{S.15}$$

We are interested in the long time steady state solution of eq. (S.15), which is time independent $P(V_1, V_2, t \to \infty) = P_{ss}(V_1, V_2)$. As the deterministic forces in eqs. (S.7)-(S.8) are linear in the variables V_1 and V_2, such a steady state solution reads

$$P_{ss}(V_1, V_2) = \frac{2\pi \mathrm{e}^{-(aV_1^2 + bV_1V_2 + cV_2^2)}}{\sqrt{-b^2 + 4ca}} \tag{S.16}$$

where the coefficients

$$\begin{aligned} a \;&=\; \frac{X\left\{C_1T_2Y + C[CR_2T_1 + T_2(C_1R_1 + CR_1 + C_2R_2)]\right\}}{2\left[Y^2T_1T_2 + C^2R_1R_2(T_1 - T_2)^2\right]}, \\ b \;&=\; -\frac{XC[(C_2 + C)R_2T_1 + (C_1 + C)R_1T_2]}{\left[Y^2T_1T_2 + C^2R_1R_2(T_1 - T_2)^2\right]}, \\ c \;&=\; \frac{X\left\{C_2T_1Y + C[CR_1T_2 + T_1(C_1R_1 + CR_2 + C_2R_2)]\right\}}{2\left[Y^2T_1T_2 + C^2R_1R_2(T_1 - T_2)^2\right]}, \end{aligned}$$

can be obtained by replacing eq. (S.16) into eq. (S.15), and by imposing the steady state condition $\partial_t P = 0$. We are furthermore interested in the unconstrained steady state probabilities $P_{1,ss}(V_1)$, and $P_{2,ss}(V_2)$, which are obtained as follows

$$P_{1,ss}(V_1) \;=\; \int \mathrm{d}V_2 P_{ss}(V_1, V_2) = \frac{\mathrm{e}^{-\frac{V_1^2}{2\sigma_1^2}}}{\sqrt{2\pi\sigma_1^2}} \tag{S.17}$$

$$P_{2,ss}(V_2) \;=\; \int \mathrm{d}V_1 P_{ss}(V_1, V_2) = \frac{\mathrm{e}^{-\frac{V_2^2}{2\sigma_2^2}}}{\sqrt{2\pi\sigma_2^2}} \tag{S.18}$$

where the variances read

$$\sigma_1^2 \;=\; \frac{T_1(C + C_2)Y + (T_2 - T_1)C^2R_1}{XY} \tag{S.19}$$

$$\sigma_2^2 \;=\; \frac{T_2(C + C_1)Y - (T_2 - T_1)C^2R_2}{XY} \tag{S.20}$$

IV. PROBABILITY DISTRIBUTION FOR THE DISSIPATED HEAT AND AVERAGE RATE

We start by noticing that the heat injected from the bath 1 is then dissipated in the bath 2 (and vice-versa), and so we expect the probability distribution of Q_1 and Q_2 to be symmetric. Thus in the following, we will only study the probability distribution of Q_1. We now proceed by introducing the joint probability distribution function of the variables V_1, V_2, and Q_1, $\Phi(V_1, V_2, Q_1, t)$ As each of these three variables evolves according to a Langevin equation, the time evolution of their PDF is described by the Fokker-Planck equation [3, 4]

$$\begin{aligned}\partial_t \Phi(V_1, V_2, Q_1, t) \;=\; & -\frac{\partial}{\partial V_1}\left(f_1\Phi\right) - \frac{\partial}{\partial V_2}\left(f_2\Phi\right) + \theta_{11}\frac{\partial^2}{\partial V_1^2}\Phi + \theta_{22}\frac{\partial^2}{\partial V_2^2}\Phi + 2\theta_{12}\frac{\partial^2}{\partial V_1 \partial V_2}\Phi \\ & - \frac{\partial}{\partial_{Q_1}}\left\{r_{11}\left[\frac{\partial}{\partial V_1}\left(V_1\Phi\right) + \left(V_1\frac{\partial}{\partial V_1}\Phi\right)\right] + 2r_{12}\frac{\partial}{\partial V_2}\left(V_1\Phi\right) + \frac{V_1^2}{R_1}\Phi\right\} \\ & + V_1^2 r_{22}\frac{\partial^2}{\partial Q_1^2}\Phi \end{aligned} \tag{S.21}$$

with

$$\begin{aligned} r_{11} &= k_1\theta_{11} + k_2\theta_{12}, \\ r_{12} &= k_1\theta_{12} + k_2\theta_{22}, \\ r_{22} &= k_1^2\theta_{11} + k_2^2\theta_{22} + 2k_1k_2\theta_{12}, \end{aligned} \tag{S.22}$$

and $k_1 = (C_1 + C)$, $k_2 = -C$. It is worth noting that the first part of the right hand side of eq. (S.21) is identical to the rhs of eq. (S.15).

We proceed by proving eq. (7) in the main text, expressing the dissipated heat rate as a function of the system parameters. We have

$$\begin{aligned} \partial_t \langle Q_1 \rangle_t &= \partial_t \int \mathrm{d}V_1\mathrm{d}V_2\mathrm{d}Q_1\; Q_1\Phi(V_1, V_2, Q_1, t) = \int \mathrm{d}V_1\mathrm{d}V_2\mathrm{d}Q_1\; Q_1\partial_t\Phi(V_1, V_2, Q, t) = -r_{11} + \frac{1}{R_1}\left\langle V_1^2 \right\rangle \\ &= \frac{C^2\Delta T}{XY}, \end{aligned} \tag{S.23}$$

where we have replaced the time derivative $\partial_t\Phi(V_1, V_2, Q, t)$ with the rhs of eq. (S.21) and used the equality $\left\langle V_1^2 \right\rangle = \sigma_1^2$, with σ_1 as given by eq. (S.19). This equation corresponds to the one given in the main text.

We can now obtain the expressions for the variance of V_1 and V_2, as introduced in the main text. Using eq.(S.23) we can express eq. (S.19) and eq. (S.20) in the following way:

$$\sigma_m^2 = \sigma_{m,\mathrm{eq}}^2 + < \dot{Q}_m > R_m \tag{S.24}$$

where $\sigma_{m,\mathrm{eq}}^2 = \frac{T_m(C+C_{m'})}{X}$ is the equilibrium value of σ_m^2 at $< \dot{Q}_m >= 0$.

V. CONSERVATION LAW

We now turn our attention to eq. (2), in the main text, and provide a formal proof for it. In order to do this, we derive a relation between the reservoir entropy change $\Delta S_{r,\tau}$ and the system dynamics. For simplicity, in the following we divide the time into small intervals Δt: let us assume that the system (the circuit in our case) is in the state $\mathbf{V} = (V_1, V_2)$ at time t, and let's denote by $\mathbf{V}' = (V_1 + \Delta V_1, V_2 + \Delta V_2)$ its state at time $t + \Delta t$. Let $\mathcal{P}_F(\mathbf{V} \to \mathbf{V}'|\mathbf{V}, t)$ be the probability that the system undergoes a transition from $\mathbf{V}$ to $\mathbf{V}'$ provided that its state at time t is $\mathbf{V}$, and let $\mathcal{P}_R(\mathbf{V}' \to \mathbf{V}|\mathbf{V}', t + \Delta t)$ be the probability of the time-reverse transition. We have

$$\begin{aligned} P_F(\mathbf{V} \to \mathbf{V}'|\mathbf{V}, t) &= \int \mathrm{d}\eta_1\mathrm{d}\eta_2\, \delta(\Delta V_1 - \Delta t \cdot (f1(V_1, V_2) + \sigma_{11}\eta_1 + \sigma_{12}\eta_2)) \\ &\quad \times\delta(\Delta V_2 - \Delta t \cdot (f_2(V_1, V_2) + \sigma_{21}\eta_1 + \sigma_{22}\eta_2))p_1(\eta_1)p_2(\eta_2), \end{aligned} \tag{S.25}$$

where $\delta(x)$ is the Dirac delta function. Given that the noises are Gaussian distributed, their probability distributions read

$$p_m(\eta_m) = \exp\left[-\frac{\eta_m^2\Delta t}{4R_m k_B T}\right]\sqrt{\frac{\Delta t}{4\pi R_m k_B T_m}} \tag{S.26}$$

and expressing the Dirac delta in Fourier space $\delta(x) = 1/(2\pi)\int \mathrm{d}q \exp(iqx)$, eq. (S.25) becomes

$$P_F(\mathbf{V} \to \mathbf{V}'|\mathbf{V}, t) = \frac{1}{(2\pi)^2}\int \mathrm{d}q_1\mathrm{d}q_2 \exp\left[\imath(q_1\Delta V_1 + q_2\Delta V_2)\right]\int \prod_m \mathrm{d}\eta_m\, \mathrm{e}^{\Delta t\left[\imath q_m(f_m + \sigma_{m1}\eta_1 + \sigma_{m2}\eta_2) - \frac{\eta_m^2}{4R_m k_B T}\right]} \tag{S.27}$$

$$\begin{aligned} &= \exp\left\{-\frac{\Delta t}{4k_B T_1 T_2}\left[C_1^2 R_1 T_2(\dot{V}_1 - f_1)^2 + C_2^2 R_2 T_1(\dot{V}_2 - f_2)^2\right.\right. \\ &\quad +2C(\dot{V}_1 - f_1 - \dot{V}_2 + f_2)(C_1 R_1 T_2(\dot{V}_1 - f_1) - C_2 R_2 T_1(\dot{V}_2 - f_2)) \\ &\quad \left.\left.+C^2(R_2 T_1 + R_1 T_2)(\dot{V}_1 - f_1 - \dot{V}_2 + f_2)^2\right]\right\}\frac{X}{4\pi k_B \Delta t}\sqrt{\frac{R_1 R_2}{T_1 T_2}}; \end{aligned} \tag{S.28}$$

where we have taken $\Delta V_m/\Delta t \simeq \dot{V}_m$, and exploited the fact that all the integrals in eq. (S.27) are Gaussian integrals. Similarly, for the reverse transition we obtain

$$\begin{aligned} P_R(\mathbf{V}' \to \mathbf{V}|\mathbf{V}', t+\Delta t) &= \int \mathrm{d}\eta_1 \mathrm{d}\eta_2\, \delta(\Delta V_1 + \Delta t(f1(V_1', V_2') + \sigma_{11}\eta_1 + \sigma_{12}\eta_2)) \\ &\quad \times \delta(\Delta V_2 + \Delta t(f_2(V_1', V_2') + \sigma_{21}\eta_1 + \sigma_{22}\eta_2)) p_1(\eta_1) p_2(\eta_2) \qquad \text{(S.29)} \\ &= \exp\left\{ -\frac{\Delta t}{4k_B T_1 T_2} \left[C_1^2 R_1 T_2 (\dot{V}_1 + f_1)^2 + C_2^2 R_2 T_1 (\dot{V}_2 + f_2)^2 \right.\right. \\ &\quad + 2C(\dot{V}_1 + f_1 - \dot{V}_2 - f_2)(C_1 R_1 T_2 (\dot{V}_1 + f_1) - C_2 R_2 T_1 (\dot{V}_2 + f_2)) \\ &\quad \left.\left. + C^2 (R_2 T_1 + R_1 T_2)(\dot{V}_1 + f_1 - \dot{V}_2 - f_2)^2 \right] \right\} \frac{X}{4\pi k_B \Delta t} \sqrt{\frac{R_1 R_2}{T_1 T_2}}. \qquad \text{(S.30)} \end{aligned}$$

We now consider the ratio between the probability of the forward and backward trajectories, and by substituting the explicit definitions of $f_1(V_1, V_2)$ and $f_2(V_1, V_2)$, as given by eqs. (S.9)-(S.10), into eqs. (S.28) and (S.30), we finally obtain

$$\log \frac{P_F(\mathbf{V} \to \mathbf{V}'|\mathbf{V}, t)}{P_R(\mathbf{V}' \to \mathbf{V}|\mathbf{V}', t+\Delta t)} = -\Delta t \left(V_1 \frac{(C_1 + C)\dot{V}_1 - C\dot{V}_2}{k_B T_1} + V_2 \frac{(C_2 + C)\dot{V}_2 - C\dot{V}_1}{k_B T_2} \right) = \Delta t \left(\frac{\dot{Q}_1}{k_B T_1} + \frac{\dot{Q}_2}{k_B T_2} \right), \qquad \text{(S.31)}$$

where we have exploited eq. (S.14) in order to obtain the rightmost equality. Thus, by taking a trajectory $\mathbf{V} \to \mathbf{V}'$ over an arbitrary time interval $[t, t+\tau]$, and by integrating the right hand side of eq. (S.31) over such time interval, we finally obtain

$$k_B \log \frac{P_F(\mathbf{V} \to \mathbf{V}'|\mathbf{V}, t)}{P_R(\mathbf{V}' \to \mathbf{V}|\mathbf{V}', t+\tau)} = \left(\frac{Q_1}{T_1} + \frac{Q_2}{T_2} \right) = \Delta S_{r,\tau} \qquad \text{(S.32)}$$

We now note that the system is in an out-of-equilibrium steady state characterized by a PDF $P_{ss}(V_1, V_2)$, and so, along any trajectory connecting two points in the phase space $\mathbf{V}$ and $\mathbf{V}'$ the following equality holds

$$\begin{aligned} \exp\left[\Delta S_{tot}/k_B\right] &= \exp\left[(\Delta S_{r,\tau} + \Delta S_{s,\tau})/k_B\right] \\ &= \frac{\mathcal{P}_F(\mathbf{V} \to \mathbf{V}'|\mathbf{V}, t) P_{ss}(\mathbf{V})}{\mathcal{P}_R(\mathbf{V}' \to \mathbf{V}|\mathbf{V}', t+\tau) P_{ss}(\mathbf{V}')}, \qquad \text{(S.33)} \end{aligned}$$

where we have exploited eq. (S.32), and the definition of $\Delta S_{s,\tau}$ in eq. (1) in the main text. Thus we finally obtain

$$\mathcal{P}_F(\mathbf{V} \to \mathbf{V}'|\mathbf{V}, t) P_{ss}(\mathbf{V}) \exp\left[-\Delta S_{tot}/k_B\right] = \mathcal{P}_R(\mathbf{V}' \to \mathbf{V}|\mathbf{V}', t+\tau) P_{ss}(\mathbf{V}') \qquad \text{(S.34)}$$

and summing up both sides over all the possible trajectories connecting any two points $\mathbf{V}$, $\mathbf{V}'$ in the phase space, and exploiting the normalization condition of the backward probability, namely

$$\sum_{\mathbf{V}', \mathbf{V}} \mathcal{P}_R(\mathbf{V}' \to \mathbf{V}|\mathbf{V}', t+\tau) P_{ss}(\mathbf{V}') = 1, \qquad \text{(S.35)}$$

one obtains eq. (2). It is worth noting that the explicit knowledge of $P_{ss}(\mathbf{V})$ is not required, in order to prove eq. (2).

Finally, we note that, from a general perspective, eqs. (S.7)-(S.8) correspond to the Langevin equations of a stochastic system, whose variables V_1 and V_2 interact through non-conservative forces, and where the white noise is correlated. Therefore our proof of eq. (S.35), and thus of eq. (2) in the main text, holds in general for systems with such characteristics.

[1] G. Cannatá, G. Scandurra, C. Ciofin,Rev. Scie. Instrum. 80,114702 (2009).
[2] R. Zwanzig, Nonequilibrium Statistical Mechanics, Oxford University Press, Oxford, 2001.
[3] A. Imparato, L. Peliti, G. Pesce, G. Rusciano, A. Sasso, *Phys. Rev. E*, **76**: 050101R (2007).
[4] H. C. Fogedby, A. Imparato, *J. Stat. Mech.* P04005 (2012).